

Multicut high dimensional model representation for reliability analysis

Rajib Chowdhury^{1a} and B.N. Rao^{*2}

¹*School of Engineering, Swansea University, Singleton Park, Swansea, UK*

²*Structural Engineering Division, Department of Civil Engineering, Indian Institute of Technology Madras, Chennai – 600 036, India*

(Received July 27, 2010, Accepted March 9, 2011)

Abstract. This paper presents a novel method for predicting the failure probability of structural or mechanical systems subjected to random loads and material properties involving multiple design points. The method involves Multicut High Dimensional Model Representation (Multicut-HDMR) technique in conjunction with moving least squares to approximate the original implicit limit state/performance function with an explicit function. Depending on the order chosen sometimes truncated Cut-HDMR expansion is unable to approximate the original implicit limit state/performance function when multiple design points exist on the limit state/performance function or when the problem domain is large. Multicut-HDMR addresses this problem by using multiple reference points to improve accuracy of the approximate limit state/performance function. Numerical examples show the accuracy and efficiency of the proposed approach in estimating the failure probability.

Keywords: structural reliability; weight function; high dimensional model representation; multiple design points; failure probability.

1. Introduction

Structural reliability assessment requires the computation of multidimensional probability integrals. Often, second moment reliability methods such as first- or second-order reliability method (FORM/SORM) (Breitung 1984, Rackwitz 2001, Adhikari 2004, Nair and Keane 2002, Adhikari 2005) are employed to predict the reliability, provided that the failure function of the structural/mechanical system can be defined in a closed form (Gavin and Yau 2008). But in reality, the failure functions are highly nonlinear and implicit in nature. Therefore, a detailed finite element (FE) modeling of the structure is necessary in combination with reliability analysis tools. FE methods for linear and nonlinear structures in conjunction with FORM/SORM have been successfully applied for structural reliability computations (Liu and Der Kiureghian 1991). But, such methods are effective for evaluating small-scale problems and for small probabilities of failure (Impollonia and Sofi 2003). In general, FORM/SORM provides fairly accurate estimate of reliability, if single design point exists on the limit state/performance function and no other important regions are found on the

*Corresponding author, Associate Professor, E-mail: bnrao@iitm.ac.in, bnrao@yahoo.com

^aNewton Fellow

limit state/performance function. The existence of multiple design points could give rise to large errors in traditional FORM/SORM approximations (Adhikari 2004, Der Kiureghian and Dakessian 1998). In that case, multipoint FORM/SORM is required for improving the reliability analysis (Der Kiureghian and Dakessian 1998).

The limitations of the conventional approximate methods (FORM/SORM) can be suitably replaced by using simulation methods (Yonezawa *et al.* 2009, Au and Beck 2001, Melchers 1989, Rubinstein 1981, Schuëller *et al.* 2004). But the main disadvantage is that, simulation methods require tremendous computational effort due to large number of deterministic structural analysis for different realizations of the random variables. Several issues related to the applicability of FORM/SORM and the efficiency of simulation methods for reliability analysis have lead many researchers to assess and improve the viability of approximate methods in the field of reliability and system safety.

Therefore there is considerable interest to investigate alternate efficient approaches for the reliability analysis of structural systems. Recently High Dimensional Model Representation (HDMR) concepts have been successfully applied to find an equivalent continuous function to replace a univariate or multivariate piece wise continuous function, rather than seeking an exact continuous function (Chowdhury *et al.* 2008) and for generation of the original limit state/performance function to predict the failure probability of structural or mechanical systems subjected to random loads and material properties with single design point (Chowdhury and Rao 2009).

This paper presents a novel method for predicting the failure probability of structural or mechanical systems subjected to random loads and material properties involving multiple design points. The method involves Multicut-HDMR technique in conjunction with Moving Least Squares (MLS) technique to approximate the original limit state/performance function with an explicit function. In this paper a weight function is presented to identify multiple reference points closer to the limit surface in a rather simplistic manner. Weight function provides an idea about multiple reference points closer to the limit surface reducing the whole sample space. After identification of reference points closer to the limit state/performance function, individual Cut-HDMR approximations of the original limit state/performance function are locally constructed at each of the identified reference points and subsequently blended to form Multicut-HDMR approximation. MCS is carried out on the approximated limit state/performance function to estimate the failure probability.

The paper is organized as follows. Section 2 presents a brief overview of HDMR and its applicability to reliability analysis. Section 3 describes the concepts of Multicut-HDMR. Section 4 describes the weight function for identification of multiple reference points closer to the limit surface. Section 5 presents approximation of the original limit state/performance function using Multicut-HDMR. Section 6 details the proposed sampling schemes. Section 7 presents the failure probability estimation by MCS using the approximate limit state/performance function generated by Multicut-HDMR. Numerical examples involving elementary mathematical functions and structural problems are presented in Section 8 to illustrate the proposed method. Comparisons have been made with alternative approximate (FORM/SORM) and simulation method to evaluate the accuracy and the computational efficiency of the present method.

2. Fundamentals of HDMR

The fundamental principle underlying the HDMR (Alis and Rabitz 2001, Li *et al.* 2001a, b, Tunga

and Demiralp 2004, 2005, Sobol 2003, Yaman and Demiralp 2009) is that, from the perspective of the output/response, the order of cooperative effects between the independent variables will die off rapidly. This assertion does not eliminate strong variable dependence or even the possibility that all the variables are important. Various sources (Alis and Rabitz 2001, Li *et al.* 2001a) of information support this point of there being limited high-order correlations. First, the variables in most systems are chosen to enter as independent entities. Second, traditional statistical analyses of system behavior have revealed that a variance and covariance analysis of the output in relation to the input variables often adequately describes the physics of the problem. These general observations lead to a dramatically reduced computational scaling when one seeks to map input-output relationships of complex systems.

Evaluating the input-output mapping of the system generates a HDMR. This is achieved by expressing system response as a hierarchical, correlated function expansion of a mathematical structure and evaluating each term of the expansion independently. One may show that system response that is a function of N input variables, $g(\mathbf{x}) = g(x_1, x_2, \dots, x_N)$, can be expressed as summands of different dimensions

$$g(\mathbf{x}) = g_0 + \sum_{i=1}^N g_i(x_i) + \sum_{1 \leq i_1 < i_2 \leq N} g_{i_1 i_2}(x_{i_1}, x_{i_2}) + \dots + \sum_{1 \leq i_1 < \dots < i_l \leq N} g_{i_1 i_2 \dots i_l}(x_{i_1}, x_{i_2}, \dots, x_{i_l}) + \dots + g_{12 \dots N}(x_1, x_2, \dots, x_N) \tag{1}$$

where g_0 is a constant term representing the mean response of $g(\mathbf{x})$. The function $g_i(x_i)$ describes the independent effect of variable x_i acting alone, although generally nonlinearly, upon the output $g(\mathbf{x})$. The function $g_{i_1 i_2}(x_{i_1}, x_{i_2})$ gives pair correlated effect of the variables x_{i_1} and x_{i_2} upon the output $g(\mathbf{x})$. The last term $g_{12 \dots N}(x_1, x_2, \dots, x_N)$ contains any residual correlated behavior over all of the system variables. Usually the higher order terms in Eq. (1) are negligible (Li *et al.* 2001a, Tunga and Demiralp 2004) such that HDMR with only low order correlations to second-order (Li *et al.* 2001a), amongst the input variables are typically adequate in describing the output behavior.

The expansion functions are determined by evaluating the input-output responses of the system relative to the defined reference point $\mathbf{c} = \{c_1, c_2, \dots, c_N\}$ along associated lines, surfaces, subvolumes, etc. (i.e., cuts) in the input variable space. This process reduces to the following relationship for the component functions in Eq. (1)

$$g_0 = g(\mathbf{c}) \tag{2}$$

$$g_i(x_i) = g(x_i, \mathbf{c}^i) - g_0 \tag{3}$$

$$g_{i_1 i_2}(x_{i_1}, x_{i_2}) = g_{i_1 i_2}(x_{i_1}, x_{i_2}, \mathbf{c}^{i_1 i_2}) - g_i(x_{i_1}) - g_{i_2}(x_{i_2}) - g_0 \tag{4}$$

where the notation $g(x_i, \mathbf{c}^i) = g(c_1, c_2, \dots, c_{i-1}, x_i, c_{i+1}, \dots, c_N)$ denotes that all the input variables are at their reference point values except x_i . The g_0 term is the output response of the system evaluated at the reference point \mathbf{c} . The higher order terms are evaluated as cuts in the input variable space through the reference point. Therefore, each first-order term $g_i(x_i)$ is evaluated along its variable axis through the reference point. Each second-order term $g_{i_1 i_2}(x_{i_1}, x_{i_2})$ is evaluated in a plane defined by the binary set of input variables x_{i_1}, x_{i_2} through the reference point, etc. The process of

subtracting off the lower order expansion functions removes their dependence to assure a unique contribution from the new expansion function.

Considering terms up to first- and second-order in Eq. (1) yields first- and second-order HDMR approximation of $g(\mathbf{x})$ as

$$\tilde{g}(\mathbf{x}) = \sum_{i=1}^N g(c_1, \dots, c_{i-1}, x_i, c_{i+1}, \dots, c_N) - (N-1)g(\mathbf{c}) \quad (5)$$

and

$$\begin{aligned} \tilde{g}(\mathbf{x}) = & \sum_{\substack{i_1=1, i_2=1 \\ i_1 < i_2}}^N g(c_1, \dots, c_{i_1-1}, x_{i_1}, c_{i_1+1}, \dots, c_{i_2-1}, x_{i_2}, c_{i_2+1}, \dots, c_N) \\ & - (N-2) \sum_{i=1}^N g(c_1, \dots, c_{i-1}, x_i, c_{i+1}, \dots, c_N) + \frac{(N-1)(N-2)}{2} g(\mathbf{c}) \end{aligned} \quad (6)$$

respectively. It can also be noted that, compared with FORM (which retains only linear terms) and SORM (which retains only quadratic terms), first- and second-order HDMR respectively, provides more accurate approximation $\tilde{g}(\mathbf{x})$ of the original limit state/performance function $g(\mathbf{x})$ (Chowdhury and Rao 2009). If first-order HDMR approximation is not sufficient second-order HDMR approximation may be adopted at the expense of additional computational cost.

3. Multicut-HDMR

The main limitation of truncated Cut-HDMR expansion is that depending on the order chosen sometimes it is unable to accurately approximate $g(\mathbf{x})$, when multiple design points exists on the limit state/performance function or when the problem domain is large (Li *et al.* 2001b). In this section, a new technique based on Multicut-HDMR is presented for approximation of the original limit state/performance function, when multiple design points exist. The basic principles of Cut-HDMR may be extended to more general cases. Multicut-HDMR is one extension where several Cut-HDMR expansions at different reference points are constructed, and the original limit state/performance function $g(\mathbf{x})$ is approximately represented not by one but by all Cut-HDMR expansions. In the present work, a new weight function is proposed for identification of multiple reference points closer to the limit surface. The theme of Multicut-HDMR approximation of the original limit state/performance function is schematically explained through Fig. 1.

Let, $\mathbf{d}^1, \mathbf{d}^2, \dots, \mathbf{d}^m$ be the m identified reference points to be closer to the limit state/performance function based on the proposed weight function presented later in Section 4. Multicut-HDMR approximation of the original limit state/performance function is based on principles of Cut-HDMR expansion, where individual Cut-HDMR expansions are constructed at different reference points $\mathbf{d}^1, \mathbf{d}^2, \dots, \mathbf{d}^m$ by taking one at a time as reference point as follows

$$\begin{aligned} g^k(\mathbf{x}) = & g_0^k + \sum_{i=1}^N g_i^k(x_i) + \sum_{1 \leq i_1 < i_2 \leq N} g_{i_1 i_2}^k(x_{i_1}, x_{i_2}) + \dots \\ & + \sum_{1 \leq i_1 < \dots < i_j \leq N} g_{i_1 i_2 \dots i_j}^k(x_{i_1}, x_{i_2}, \dots, x_{i_j}) + \dots + g_{12 \dots N}^k(x_1, x_2, \dots, x_N); \quad k = 1, 2, \dots, m \end{aligned} \quad (7)$$

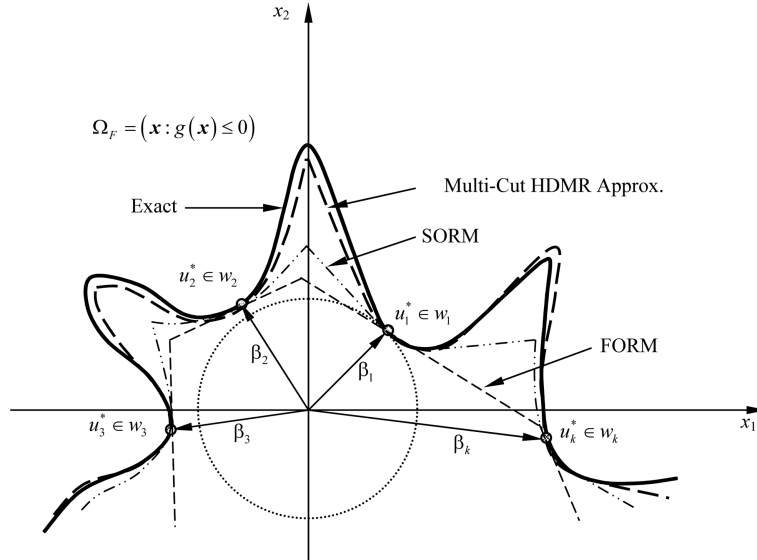


Fig. 1 Concept of Multi-Cut HDMR approximation of original limit state/performance function in conjunction with the weight function

The original limit state/performance function $g(\mathbf{x})$ is approximately represented not by one but by blending all locally constructed m individual Cut-HDMR expansions as follows

$$g(\mathbf{x}) \cong \sum_{k=1}^m \lambda_k(\mathbf{x}) \left[g_0^k + \sum_{i=1}^N g_i^k(x_i) + \dots + g_{12\dots N}^k(x_1, x_2, \dots, x_N) \right] \quad (8)$$

The coefficients $\lambda_k(\mathbf{x})$ possess the properties

$$\lambda_k(\mathbf{x}) = \begin{cases} 1 & \text{if } \mathbf{x} \text{ is in any cut subvolume of the } k\text{-th reference point expansions} \\ 0 & \text{if } \mathbf{x} \text{ is in any cut subvolume of other reference point expansions} \end{cases} \quad (9)$$

and

$$\sum_{k=1}^m \lambda_k(\mathbf{x}) = 1 \quad (10)$$

There are a variety of choices to define $\lambda_k(\mathbf{x})$. In the present study, the metric distance $\alpha_k(\mathbf{x})$ from any sample point to the reference point \mathbf{d}^k ; $k = 1, 2, \dots, m$

$$\alpha_k(\mathbf{x}) = \left[\sum_{i=1}^N (x_i - d_i^k)^2 \right]^{1/2}; \quad d_i^k \equiv k\text{-th reference point} \quad (11)$$

is used to define

$$\lambda_k(\mathbf{x}) = \frac{\bar{\lambda}_k(\mathbf{x})}{\sum_{s=1}^M \bar{\lambda}_s(\mathbf{x})} \quad (12)$$

where

$$\bar{\lambda}_k(\mathbf{x}) = \prod_{\substack{s=1 \\ s \neq k}}^m \alpha_s(\mathbf{x}) \quad (13)$$

The coefficients $\lambda_k(\mathbf{x})$ determine the contribution of each locally approximated function to the global function. The properties of the coefficients $\lambda_k(\mathbf{x})$ imply that the contribution of all other Cut-HDMR expansions vanish except one when \mathbf{x} is located on any cut line, plane, or higher dimensional ($\leq l$) sub-volumes through that reference point, and then the Multicut-HDMR expansion reduces to single point Cut-HDMR expansion. As mentioned above, the l -th order Cut-HDMR approximation does not have error when \mathbf{x} is located on these sub-volumes. When m Cut-HDMR expansions are used to construct a Multicut-HDMR expansion, the error free region in input \mathbf{x} space is m times that for a single reference point Cut-HDMR expansion. Therefore, the accuracy will be improved.

Therefore, first- and second-order Multicut-HDMR approximation of the original limit state/performance function $g(\mathbf{x})$ with m reference points can be expressed as

$$\tilde{g}(\mathbf{x}) \cong \sum_{k=1}^m \lambda_k(\mathbf{x}) \left(\sum_{i=1}^N g^k(d_1^k, \dots, d_{i-1}^k, x_i, d_{i+1}^k, \dots, d_N^k) \right) - (N-1)g^k(\mathbf{d}^k) \quad (14)$$

and

$$\tilde{g}(\mathbf{x}) \cong \sum_{k=1}^m \lambda_k(\mathbf{x}) \left[\begin{array}{l} \sum_{\substack{i_1=1, i_2=1 \\ i_1 < i_2}}^N g^k(d_1^k, \dots, d_{i_1-1}^k, x_{i_1}, d_{i_1+1}^k, \dots, d_{i_2-1}^k, x_{i_2}, d_{i_2+1}^k, \dots, d_N^k) \\ - (N-2) \sum_{i=1}^N g^k(d_1^k, \dots, d_{i-1}^k, x_i, d_{i+1}^k, \dots, d_N^k) + \frac{(N-1)(N-2)}{2} g^k(\mathbf{d}^k) \end{array} \right] \quad (15)$$

respectively.

4. Weight function for identification of multiple reference points

The most important part of Multicut-HDMR approximation of the original limit state/performance function is identification of multiple reference points closer to the limit state/performance function. The proposed weight function is similar to that used by other researcher (Kaymaz and McMahon 2005) for weighted regression analysis. Among the limit state/performance function responses at all sample points, the most likelihood point is selected based on closeness to zero value, which indicates that particular sample point is close to the limit state/performance function.

In this study two types of procedures are adopted for identification of reference points closer to the limit state/performance function, namely: (1) first-order method, and (2) second-order method. The procedure for identification of reference points closer to the limit state/performance function using first-order method proceeds as follows: (a) $n(=3, 5, 7$ or $9)$ equally spaced sample points $\mu_i - (n-1)\sigma_i/2, \mu_i - (n-3)\sigma_i/2, \dots, \mu_i, \dots, \mu_i + (n-3)\sigma_i/2, \mu_i + (n-1)\sigma_i/2$ are deployed along each of the variable axis x_i with mean μ_i and standard deviation σ_i , through an initial reference point. First-order method for identification of multiple reference points closer to the limit state/

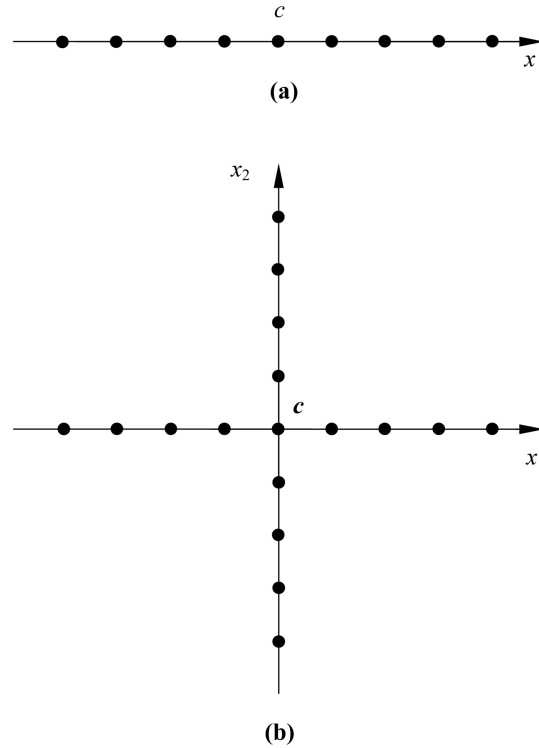


Fig. 2 Sampling scheme for first-order HDMR (a) for a function having one variable (x), and (b) for a function having two variables (x_1 and x_2)

performance function, for a function having one variable (x) and two variables (x_1 and x_2) is shown in Figs. 2(a) and 2(b) respectively. Initial reference point is taken as mean value of the random variables; (b) The limit state/performance function is evaluated at each sample point; (c) Using the limit state/performance function responses at all sample points, the weight corresponding to each sample point is evaluated using the following weight function

$$w^I = \exp\left(-\frac{(g(c_1, \dots, c_{i-1}, x_i, c_{i+1}, \dots, c_N) - g(\mathbf{x}))|_{\min}}{|g(\mathbf{x})|_{\min}}\right) \quad (16)$$

Second-order method of identification of reference points closer to the limit state/performance function, proceeds as follows: (a) A regular grid is formed by taking $n(=3, 5, 7$ or $9)$ equally spaced sample points $\mu_{i_1} - (n-1)\sigma_{i_1}/2, \mu_{i_1} - (n-3)\sigma_{i_1}/2, \dots, \mu_{i_1}, \dots, \mu_{i_1} + (n-3)\sigma_{i_1}/2, \mu_{i_1} + (n-1)\sigma_{i_1}/2$ along x_{i_1} axis with mean μ_{i_1} and standard deviation σ_{i_1} , and $n(=3, 5, 7$ or $9)$ equally spaced sample points $\mu_{i_2} - (n-1)\sigma_{i_2}/2, \mu_{i_2} - (n-3)\sigma_{i_2}/2, \dots, \mu_{i_2}, \dots, \mu_{i_2} + (n-3)\sigma_{i_2}/2, \mu_{i_2} + (n-1)\sigma_{i_2}/2$ along x_{i_2} axis with mean μ_{i_2} and standard deviation σ_{i_2} , through an initial reference point. Second-order method for identification of multiple reference points closer to the limit state/performance function, for a function having two variables (x_1 and x_2) is shown in Fig. 3. Initial reference point is taken as mean value of the random variables; (b) The limit state/performance function is evaluated at each sample point; (c) Using the limit state/performance function responses at all sample points, the weight corresponding to each sample point is evaluated using the following weight function

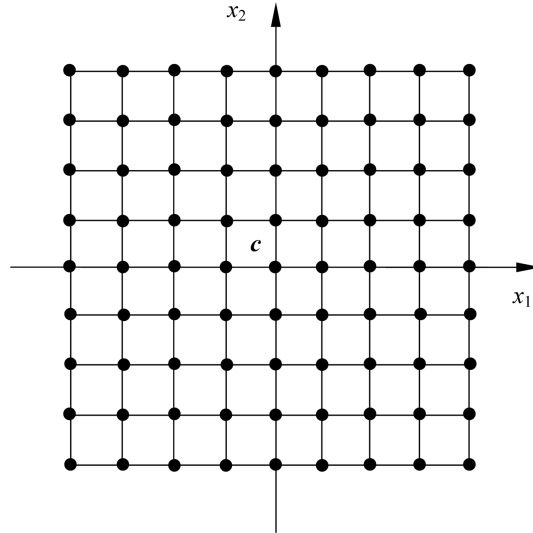


Fig. 3 Sampling scheme for second-order HDMR for a function having two variables (x_1 and x_2)

$$w^H = \exp\left(-\frac{(g(c_1, \dots, c_{i-1}, x_i, c_{i+1}, \dots, c_{i_2-1}, x_i, c_{i_2+1}, \dots, c_N) - g(\mathbf{x})|_{\min})}{|g(\mathbf{x})|_{\min}}\right) \quad (17)$$

Sample points $\mathbf{d}^1, \mathbf{d}^2, \dots, \mathbf{d}^m$ with maximum weight are selected as reference points closer to the limit state/performance function, for construction of m individual Cut-HDMR approximations of the original limit state/performance function locally.

5. Limit state/performance function generation

Multicut-HDMR in Eq. (8) is exact along any of the cuts through m reference points $\mathbf{d}^1, \mathbf{d}^2, \dots, \mathbf{d}^m$, and the output response $g(\mathbf{x})$ at a point \mathbf{x} off of the cuts can be obtained as follows:

Step 1: Interpolate each of the low dimensional individual Cut-HDMR expansion terms with respect to the input values of the point \mathbf{x} . For example, consider the first-order component function $g^k(x_i, \mathbf{d}^k) = g^k(d_1^k, \dots, d_{i-1}^k, x_i, d_{i+1}^k, \dots, d_N^k)$ for k -th reference point. If for $x_i = x_i^j$, n function values

$$g^k(x_i^j, \mathbf{d}^k) = g^k(d_1^k, \dots, d_{i-1}^k, x_i^j, d_{i+1}^k, \dots, d_N^k); \quad j = 1, 2, \dots, n \quad (18)$$

are given at $n(=3, 5, 7 \text{ or } 9)$ equally spaced sample points $\mu_i - (n-1)\sigma_i/2, \mu_i - (n-3)\sigma_i/2, \dots, \mu_i, \dots, \mu_i + (n-3)\sigma_i/2, \mu_i + (n-1)\sigma_i/2$ along the variable axis x_i with mean μ_i and standard deviation σ_i , the function value for arbitrary x_i can be obtained by the MLS interpolation (Lancaster and Salkauskas 1986) as

$$g^k(x_i, \mathbf{d}^k) = \sum_{j=1}^n \phi_j^k(x_i) g^k(d_1^k, \dots, d_{i-1}^k, x_i^j, d_{i+1}^k, \dots, d_N^k) \quad (19)$$

where

$$\begin{Bmatrix} g^{rk}(x_i^1, \mathbf{d}^i) \\ \vdots \\ g^{rk}(x_i^n, \mathbf{d}^i) \end{Bmatrix} = \begin{bmatrix} \phi_1(x_i^1) & \phi_2(x_i^1) & \cdots & \phi_n(x_i^1) \\ \vdots & \vdots & \vdots & \vdots \\ \phi_1(x_i^n) & \phi_2(x_i^n) & \cdots & \phi_n(x_i^n) \end{bmatrix}^{-1} \begin{Bmatrix} g^k(x_i^1, \mathbf{d}^i) \\ \vdots \\ g^k(x_i^n, \mathbf{d}^i) \end{Bmatrix} \quad (20)$$

Similarly, consider the second-order component function. $g^k(x_{i_1}, x_{i_2}, \mathbf{d}^{k^{i_1 i_2}}) = g^k(d_1^k, \dots, d_{i_1-1}^k, x_{i_1}, d_{i_1+1}^k, \dots, d_{i_2-1}^k, x_{i_2}, d_{i_2+1}^k, \dots, d_N^k)$. If for $x_{i_1} = x_{i_1}^{j_1}$, and $x_{i_2} = x_{i_2}^{j_2}$, n^2 function values

$$g^k(x_{i_1}^{j_1}, x_{i_2}^{j_2}, \mathbf{d}^{k^{i_1 i_2}}) = g^k(d_1^k, \dots, d_{i_1-1}^k, x_{i_1}^{j_1}, d_{i_1+1}^k, \dots, d_{i_2-1}^k, x_{i_2}^{j_2}, d_{i_2+1}^k, \dots, d_N^k) \quad (21)$$

$$j_1 = 1, 2, \dots, n, \quad j_2 = 1, 2, \dots, n$$

are given on a grid formed by taking $n(=3, 5, 7$ or $9)$ equally spaced sample points $\mu_{i_1} - (n-1)\sigma_{i_1}/2, \mu_{i_1} - (n-3)\sigma_{i_1}/2, \dots, \mu_{i_1}, \dots, \mu_{i_1} + (n-3)\sigma_{i_1}/2, \mu_{i_1} + (n-1)\sigma_{i_1}/2$ along x_{i_1} axis with mean μ_{i_1} and standard deviation σ_{i_1} , and $n(=3, 5, 7$ or $9)$ equally spaced sample points $\mu_{i_2} - (n-1)\sigma_{i_2}/2, \mu_{i_2} - (n-3)\sigma_{i_2}/2, \dots, \mu_{i_2}, \dots, \mu_{i_2} + (n-3)\sigma_{i_2}/2, \mu_{i_2} + (n-1)\sigma_{i_2}/2$ along x_{i_2} axis with mean μ_{i_2} and standard deviation σ_{i_2} , the function value for arbitrary (x_{i_1}, x_{i_2}) can be obtained by the MLS interpolation as

$$g^k(x_{i_1}, x_{i_2}, \mathbf{d}^{k^{i_1 i_2}}) = \sum_{j_1=1}^n \sum_{j_2=1}^n \phi_{j_1 j_2}(x_{i_1}, x_{i_2}) g^k(d_1^k, \dots, d_{i_1-1}^k, x_{i_1}^{j_1}, d_{i_1+1}^k, \dots, d_{i_2-1}^k, x_{i_2}^{j_2}, d_{i_2+1}^k, \dots, d_N^k) \quad (22)$$

where

$$\begin{Bmatrix} g^{rk}(x_{i_1}^1, x_{i_2}^1, \mathbf{d}^{i_1 i_2}) \\ \vdots \\ g^{rk}(x_{i_1}^1, x_{i_2}^n, \mathbf{d}^{i_1 i_2}) \\ \vdots \\ g^{rk}(x_{i_1}^n, x_{i_2}^n, \mathbf{d}^{i_1 i_2}) \end{Bmatrix} = \begin{bmatrix} \phi_{11}(x_{i_1}^1, x_{i_2}^1) & \cdots & \phi_{1n}(x_{i_1}^1, x_{i_2}^1) & \cdots & \phi_{mn}(x_{i_1}^1, x_{i_2}^1) \\ \vdots & \vdots & \vdots & \vdots & \vdots \\ \phi_{11}(x_{i_1}^1, x_{i_2}^n) & \cdots & \phi_{1n}(x_{i_1}^1, x_{i_2}^n) & \cdots & \phi_{mn}(x_{i_1}^1, x_{i_2}^n) \\ \vdots & \vdots & \vdots & \vdots & \vdots \\ \phi_{11}(x_{i_1}^n, x_{i_2}^n) & \cdots & \phi_{1n}(x_{i_1}^n, x_{i_2}^n) & \cdots & \phi_{mn}(x_{i_1}^n, x_{i_2}^n) \end{bmatrix}^{-1} \begin{Bmatrix} g^k(x_{i_1}^1, x_{i_2}^1, \mathbf{d}^{i_1 i_2}) \\ \vdots \\ g^k(x_{i_1}^1, x_{i_2}^n, \mathbf{d}^{i_1 i_2}) \\ \vdots \\ g^k(x_{i_1}^n, x_{i_2}^n, \mathbf{d}^{i_1 i_2}) \end{Bmatrix} \quad (23)$$

The interpolation functions $\phi_j(x_i)$ and $\phi_{j_1 j_2}(x_{i_1}, x_{i_2})$ can be obtained using the MLS interpolation scheme.

By using Eq. (19), $g_i^k(x_i)$ can be generated if n function values are given at corresponding sample points. Similarly, by using Eq. (21), $g_{i_1 i_2}^k(x_{i_1}, x_{i_2})$ can be generated if n^2 function values at corresponding sample points are given. The same procedure shall be repeated for all the first-order component functions, i.e., $g_i^k(x_i); i = 1, 2, \dots, N; k = 1, 2, \dots, m$ and the second-order component functions, i.e., $g_{i_1 i_2}^k(x_{i_1}, x_{i_2}); i_1, i_2 = 1, 2, \dots, N; k = 1, 2, \dots, m$.

Step 2: Sum the interpolated values of individual Cut-HDMR expansion terms from zeroth-order to the highest order retained in keeping with the desired accuracy and blend all locally constructed m individual Cut-HDMR expansions using the coefficients $\lambda_k(\mathbf{x})$. This leads to first- and second-order Multicut-HDMR approximation of the original limit state/performance function $g(\mathbf{x})$ with m

reference points closer to the limit state/performance function as

$$\tilde{g}(\mathbf{x}) \cong \sum_{k=1}^m \lambda_k(\mathbf{x}) \left[\sum_{i=1}^N \sum_{j=1}^n \phi_j^k(x_i) g^{rk}(d_1^k, \dots, d_{i-1}^k, x_i^j, d_{i+1}^k, \dots, d_N^k) - (N-1) g^k(\mathbf{d}^k) \right] \quad (24)$$

and

$$\tilde{g}(\mathbf{x}) \cong \sum_{k=1}^m \lambda_k(\mathbf{x}) \left[\sum_{\substack{i_1=1, i_2=1 \\ i_1 < i_2}}^N \sum_{j_1=1}^n \sum_{j_2=1}^n \phi_{j_1 j_2}^k(x_{i_1}, x_{i_2}) g^{rk}(d_1^k, \dots, d_{i_1-1}^k, x_{i_1}^{j_1}, d_{i_1+1}^k, \dots, d_{i_2-1}^k, x_{i_2}^{j_2}, d_{i_2+1}^k, \dots, d_N^k) \right. \\ \left. - (N-2) \sum_{i=1}^N \sum_{j=1}^n \phi_j^k(x_i) g^{rk}(d_1^k, \dots, d_{i-1}^k, x_i^j, d_{i+1}^k, \dots, d_N^k) + \frac{(N-1)(N-2)}{2} g^k(\mathbf{d}^k) \right] \quad (25)$$

respectively.

In contrast to FORM (which retains only linear terms) and SORM (which retains only quadratic terms), first- and second-order Multicut-HDMR respectively, provides more accurate approximation $\tilde{g}(\mathbf{x})$ of the original limit state/performance function $g(\mathbf{x})$. If first-order Multicut-HDMR approximation is not sufficient second-order Multicut-HDMR approximation may be adopted at the expense of additional computational cost.

If n is the number of sample points taken along each of the variable axis and s is the order of the component function considered, starting from zeroth-order to l -th order and m is the number of identified reference points closer to the limit state/performance function., then total number of function evaluation for interpolation purpose is given by, $m \sum_{s=0}^l (N!(n-1)^s)/((N-s)!s!)$ which grows polynomially with n and s . As a few low order component functions of HDMR are used, the sample savings due to Multicut-HDMR are significant compared to traditional sampling. Hence uncertainty analysis using Multicut-HDMR relies on an accurate reduced model being generated with a small number of full model simulations. An arbitrarily large sample Monte Carlo simulation (MCS) can be performed on the outputs approximated by Multicut-HDMR which result in the same distributions as obtained through the MCS of the full model. The tremendous computational savings result from just having to perform interpolation instead of full model simulations for output determination.

6. Sampling schemes

For approximation of the original limit state/performance function using Eqs. (24) and (25) four types of sampling schemes, namely FF, FS, SF and SS, are adopted in this study which are schematically illustrated in Figs. 4(a), (b) and Figs. 5(a), (b). Fig. 4(a) shows FF sampling scheme involving first-order method of identification of reference points closer to the limit state/performance function (adopting sampling scheme shown in Figs. 2(a) or 2(b)) and blending of locally constructed individual first-order HDMR approximations of the original limit state/performance function (adopting sampling scheme shown in Figs. 2(a) or 2(b)) at different identified reference points $\mathbf{d}^1, \mathbf{d}^2, \dots, \mathbf{d}^m$ using the coefficients $\lambda_k(\mathbf{x})$ to form Multicut-HDMR approximation $\tilde{g}(\mathbf{x})$ of $g(\mathbf{x})$ using Eq. (24). Fig. 4(b) shows FS sampling scheme involving first-order method of

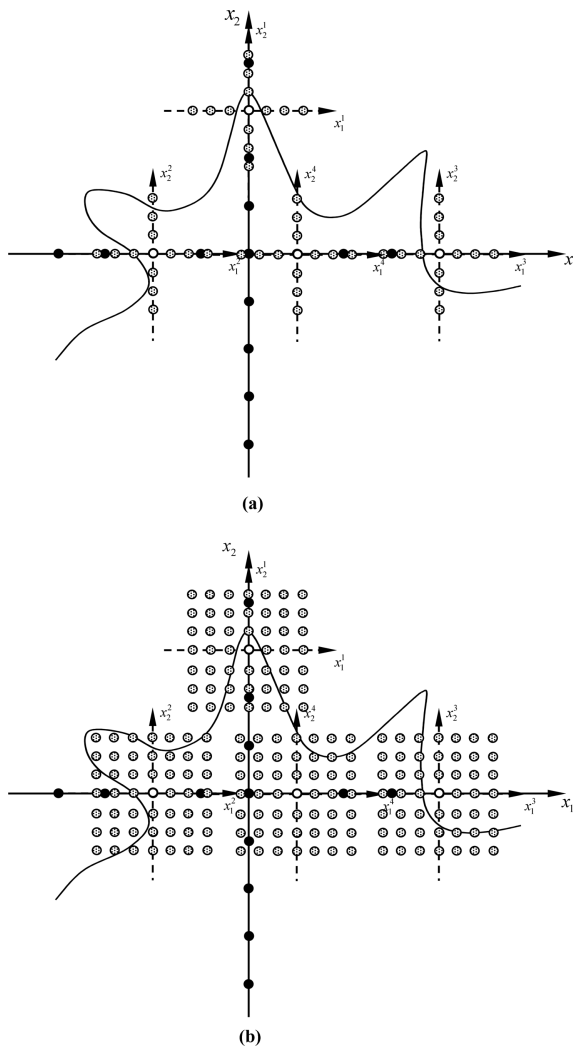


Fig. 4 Multi-Cut HDMR approximation of original limit state/performance function; with (a) FF sampling scheme and (b) FS sampling scheme

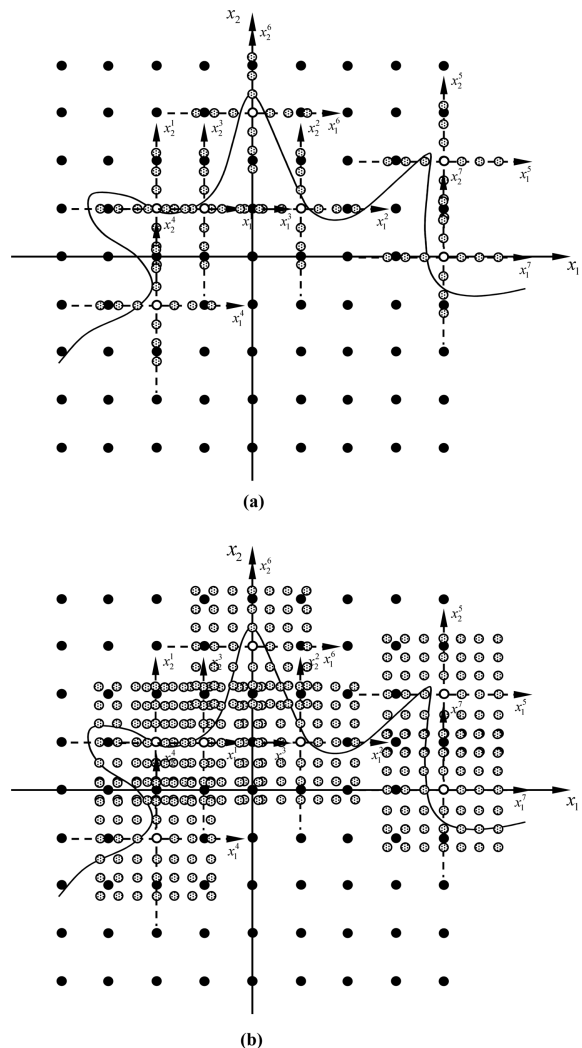


Fig. 5 Multi-Cut HDMR approximation of original limit state/performance function; with (a) SF sampling scheme and (b) SS sampling scheme

identification of reference points closer to the limit state/performance function (adopting sampling scheme shown in Figs. 2(a) or 2(b)) and blending of locally constructed individual second-order HDMR approximations of the original limit state/performance function (adopting sampling scheme shown in Fig. 3) at different identified reference points $\mathbf{d}^1, \mathbf{d}^2, \dots, \mathbf{d}^m$ using the coefficients $\lambda_k(\mathbf{x})$ to form Multicut-HDMR approximation $\tilde{g}(\mathbf{x})$ of $g(\mathbf{x})$ using Eq. (25). Fig. 5(a) SF sampling scheme involving second-order method of identification of reference points closer to the limit state/performance function (adopting sampling scheme shown in Fig. 3) and blending of locally constructed individual first-order HDMR approximations of the original limit state/performance function (adopting sampling scheme shown in Figs. 2(a) or 2(b)) at different identified reference points $\mathbf{d}^1, \mathbf{d}^2, \dots, \mathbf{d}^m$ using the coefficients $\lambda_k(\mathbf{x})$ to form Multicut-HDMR approximation $\tilde{g}(\mathbf{x})$ of

$g(\mathbf{x})$ using Eq. (24). Fig. 5(b) SS sampling scheme involving second-order method of identification of reference points closer to the limit state/performance function (adopting sampling scheme shown in Fig. 3) and blending of locally constructed individual second -order HDMR approximations of the original limit state/performance function (adopting sampling scheme shown in Fig. 3) at different identified reference points $\mathbf{d}^1, \mathbf{d}^2, \dots, \mathbf{d}^m$ using the coefficients $\lambda_k(\mathbf{x})$ to form Multicut-HDMR approximation $\tilde{g}(\mathbf{x})$ of $g(\mathbf{x})$ using Eq. (25).

7. Failure probability estimation

The failure probability P_F can be easily estimated by performing MCS on first- or second-order Multicut-HDMR approximation $\tilde{g}(\mathbf{x})$ of the original limit state/performance function $g(\mathbf{x})$ (obtained by using Eqs. (24) and (25) and adopting any of four types of sampling schemes discussed above) and is given by

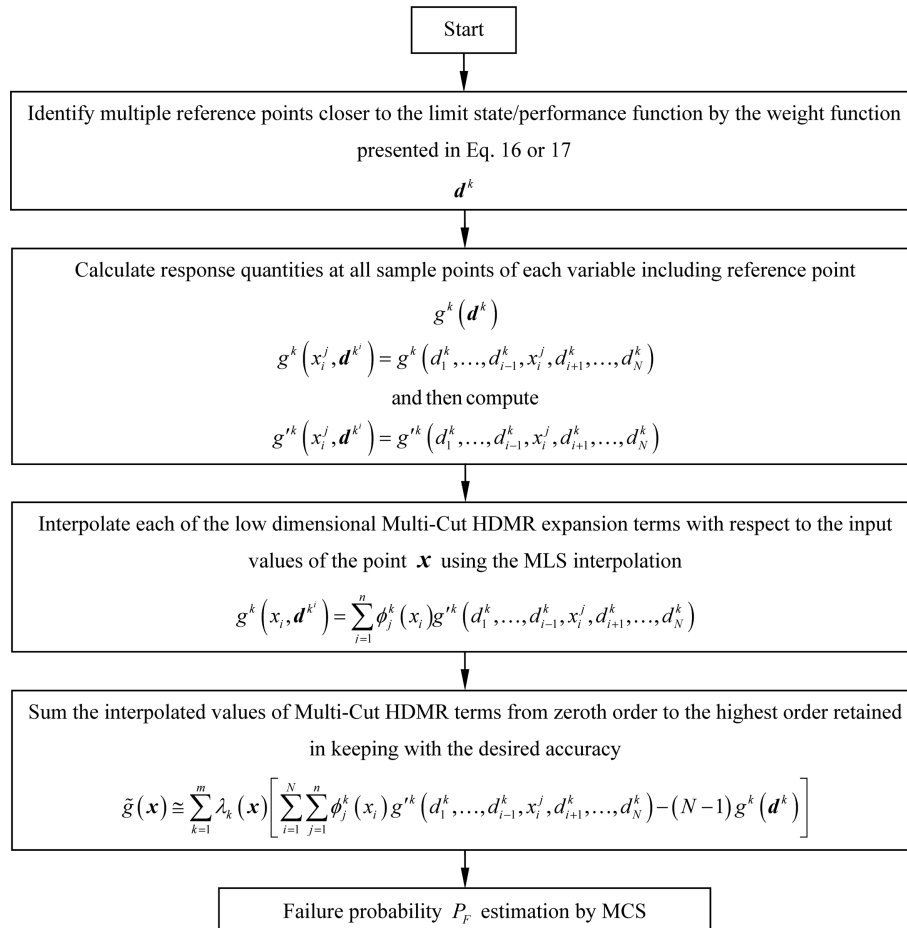


Fig. 6 Flowchart of failure probability P_F estimation using first-order Multi-Cut HDMR approximation of original limit state/performance function

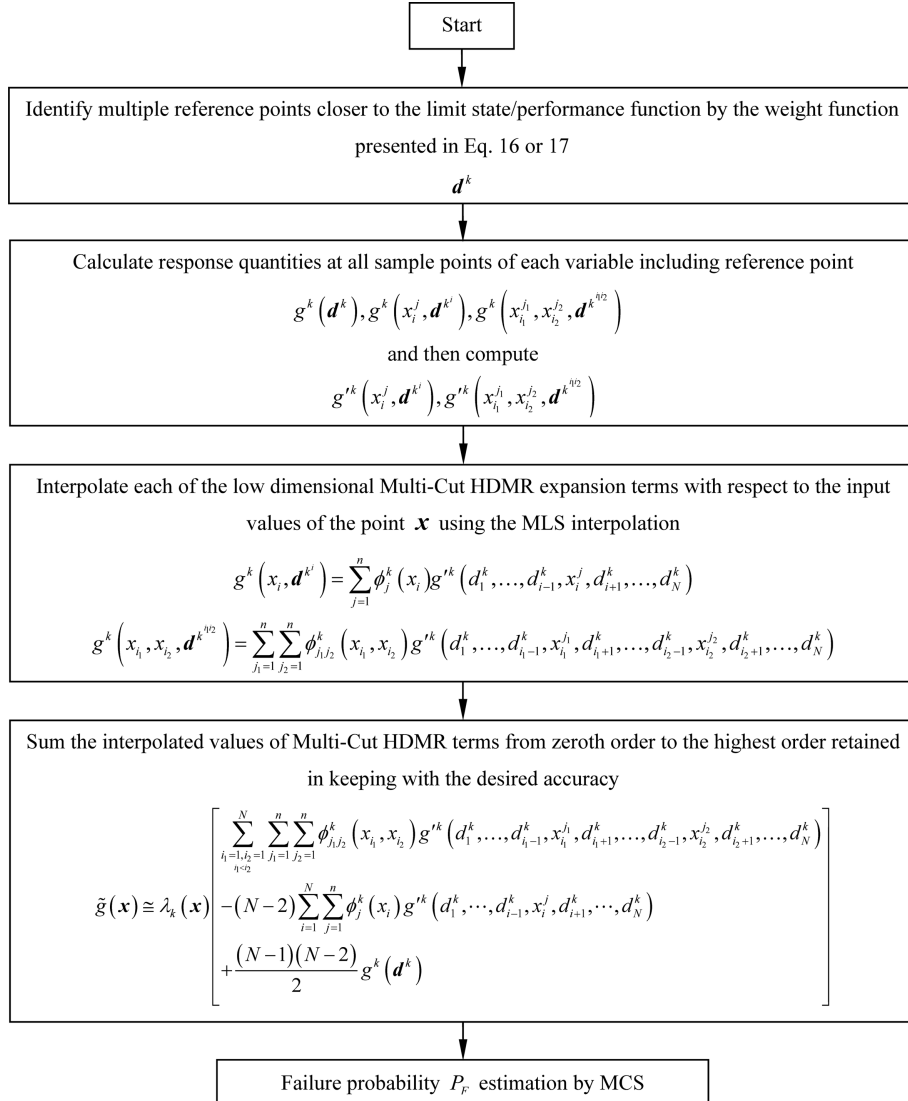


Fig. 7 Flowchart of failure probability P_F estimation using second-order Multi-Cut HDMR approximation of original limit state/performance function

$$P_F = \frac{1}{N_S} \sum_{s_i=1}^{N_S} I[\tilde{g}(\mathbf{x}^i) < 0] \quad (26)$$

where \mathbf{x}^i is i th realization of \mathbf{X} , N_S is the sampling size, $I[\cdot]$ is a deciding function of fail or safe state such that $I = 1$, if $\tilde{g}(\mathbf{x}^i) < 0$ otherwise zero. A flow diagram for the limit state/performance function generation using first-order Multicut-HDMR approximation with multiple reference points closer to the limit state/performance function and the failure probability P_F estimation by MCS is shown in Fig. 6. Likewise, computational flow for the limit state/performance function generation using second-order Multicut-HDMR approximation with multiple reference points closer to the limit

state/performance function and the failure probability P_F estimation by MCS is shown in Fig. 7. The reliability index β corresponding to the failure probability P_F can be obtained by

$$\beta = -\Phi^{-1}(P_F) \quad (27)$$

where $\Phi(\bullet)$ is the cumulative distribution function of a standard Gaussian random variable.

8. Numerical examples

Three numerical examples involving explicit performance functions from mathematical problems (Examples 1 and 2) and performance functions from structural or solid-mechanics problems (Example 3) are presented to illustrate the proposed method. To evaluate the accuracy and the efficiency of the present method, comparisons of the estimated failure probability P_F using Multicut-HDMR (given by Eqs. (24) and (25) and adopting any of four types of sampling schemes discussed above) based and second-order HDMR (given by Eq. (6)) approximation of the original limit state/performance function, have been made with FORM/SORM and direct MCS. The coefficient of variation δ of the estimated failure probability P_F by direct MCS for the sampling size N_S considered, is computed using

$$\delta = \sqrt{\frac{(1-P_F)}{N_S P_F}} \quad (28)$$

When comparing computational efforts by various methods in evaluating the failure probability P_F , the number of original limit state/performance function evaluations is chosen as the primary comparison tool in this paper. This is because of the fact that, number of function evaluations indirectly indicates the CPU time usage. For direct MCS, number of original function evaluations is same as the sampling size. While evaluating the failure probability P_F through direct MCS, CPU time is more because it involves number of repeated actual finite-element analysis. However, in the present method MCS is conducted in conjunction with the proposed approximation of the original limit state/performance function based on Multicut-HDMR. Here, although the same sampling size as in direct MCS is considered, the number of original function evaluation is very less. Hence, the computational effort expressed in terms of function evaluations alone should be carefully interpreted for problems involving explicit functions. In all the sampling schemes the initial reference point \mathbf{c} is taken as mean values of the random variables. In all the numerical examples presented same value of n is used for identification of multiple reference points closer to the limit state/performance function and subsequently for construction of local individual Cut-HDMR expansions, even though different values of n could be adopted.

8.1 Example 1: parabolic performance function

The limit state/performance function considered is a parabola of the form

$$g(\mathbf{x}) = 7 - x_1^2 - x_2 \quad (29)$$

with two independent standard normal variables x_1 and x_2 . As shown in Fig. 8 the limit state

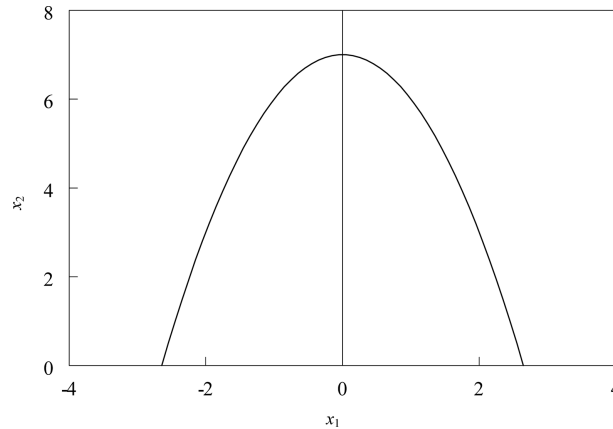


Fig. 8 Limit state function of Example 1

Table 1 Identification of multiple design points for Example 1 with FF sampling

Sample points		Response	Minimum response	w^j
x_1	x_2	$g(\mathbf{x})$	$g(\mathbf{x}) _{\min}$	
-2.00	0.00	3.00		1.00
-1.00	0.00	6.00		0.37
0.00	0.00	7.00		0.26
1.00	0.00	6.00		0.37
2.00	0.00	3.00		1.00
0.00	-2.00	9.00	3	0.14
0.00	-1.00	8.00		0.19
0.00	0.00	7.00		0.26
0.00	1.00	6.00		0.37
0.00	2.00	5.00		0.51

function given by Eq. (29) is symmetric about x_2 and has two design points. The two actual design points obtained using recursive quadratic programming (RQP) algorithm (Arora 2004) are (2.54, 0.49) and (-2.54, 0.49) with reliability indices $\beta_1 = \beta_2 = 2.588$.

Table 1 illustrates computational details and identification of reference points $\mathbf{d}^1, \mathbf{d}^2, \dots, \mathbf{d}^m$ using FF sampling scheme with five equally spaced sample points ($n = 5$) along each of the variable axis. Table 1 shows two reference points (2, 0) and (-2, 0) closer to the limit state/performance function producing maximum weight (obtained using Eq. (16)). After identification of the two reference points (2, 0) and (-2, 0), local individual first-order HDMR approximations of the original limit state/performance function are constructed at the two reference points by deploying five equally spaced sample points ($n = 5$) along each of the variable axis. Local approximations of the original limit state/performance function are blended together (using Eq. (24)) to form global approximation. Comparison of the failure probability estimation by different methods is presented in Table 2. A sampling size $N_S = 10^6$ is considered in direct MCS to evaluate the failure probability P_F and the coefficient of variation (COV) of P_F corresponding to this sampling size is 0.01 (computed using Eq. (28)).

Table 2 Estimation of failure probability for parabolic function in Example 1

Method	Failure probability	Number of function evaluation ^(a)
FORM	0.004823	41
SORM (Adhikari 2004)	0.004926	116
Direct Monte Carlo simulation	0.009747	10 ⁶
Multicut-HDMR Approximation: FF sampling	0.009747	21
Multicut-HDMR Approximation: FS sampling	0.009747	45
Multicut-HDMR Approximation: SF sampling	0.009747	33
Multicut-HDMR Approximation: SS sampling	0.009747	45
Second-order HDMR	0.009747	25

^(a)Total number of times the original performance function is calculated.

^(b)Curvature fitting method is used to approximate the required curvatures of the limit-state surface.

Table 3 Identification of multiple design points for Example 1 with SF sampling

Sample points		Response	Minimum response	w^H
x_1	x_2	$g(\mathbf{x})$	$g(\mathbf{x}) _{\min}$	
-2	-2	5	1	0.02
-1	-2	8		0.00
0	-2	9		0.00
1	-2	8		0.00
2	-2	5		0.02
-2	-1	4		0.05
-1	-1	7		0.00
0	-1	8		0.00
1	-1	7		0.00
2	-1	4		0.05
-2	0	3		0.14
-1	0	6		0.01
0	0	7		0.00
1	0	6		0.01
2	0	3		0.14
-2	1	2		0.37
-1	1	5		0.02
0	1	6		0.01
1	1	5		0.02
2	1	2		0.37
-2	2	1		1.00
-1	2	4		0.05
0	2	5		0.02
1	2	4		0.05
2	2	1		1.00

Effect of FS sampling scheme on the estimated failure probability P_F is studied by constructing local individual second-order HDMR approximations of the original limit state/performance function at the two reference points $(2, 0)$ and $(-2, 0)$ by forming a regular grid around the two reference points with five equally spaced sample points ($n=5$) along each of the variable axis. Local approximations of the original limit state/performance function constructed at the two reference points are blended together (using Eq. (25)) to make a global approximation. Table 2 also shows the failure probability P_F estimate obtained by the proposed method based on FS sampling scheme.

Table 3 presents computational details and identification of reference points closer to the limit state/performance function using SF sampling scheme. Five equally spaced sample points $n = 5$ along each of the variable axis are deployed to form a regular grid through the initial reference point \mathbf{c} . Table 3 shows two reference points $(2, 2)$ and $(-2, 2)$ closer to the limit state/performance function producing maximum weight (obtained using Eq. (17)). After identification of the two reference points $(2, 2)$ and $(-2, 2)$, local individual first-order HDMR approximations of the original limit state/performance function are constructed at the two reference points by deploying five equally spaced sample points ($n = 5$) along each of the variable axis. Local approximations of the original limit state/performance function are blended together (using Eq. (24)) to form global approximation. The failure probability P_F estimate obtained by the proposed method based on SF sampling scheme is shown in Table 2.

In addition, effect of SS sampling scheme on the estimated failure probability P_F is studied by constructing local individual second-order HDMR approximations of the original limit state/performance function at the two reference points $(2, 2)$ and $(-2, 2)$ by forming a regular grid around the two reference points with five equally spaced sample points ($n = 5$) along each of the variable axis. Local approximations of the original limit state/performance function constructed at the two reference points are blended together (using Eq. (25)) to make a global approximation. Table 2 also shows the failure probability P_F estimate obtained by the proposed method based on SS sampling scheme.

In an effort to reduce the computational effort in FF, FS, SF and SS sampling schemes without compromising on the accuracy of the failure probability estimate second-order HDMR approximation of the original limit state/performance function (refer Eq. (6)) is constructed using a regular grid formed with five equally spaced sample points ($n = 5$) along each of the variable axis with reference point taken as the mean value of the random variables. Table 2 also shows the failure probability P_F value obtained using second-order HDMR approximation (refer Eq. (60)) and the associated computational effort in terms of number of function evaluations. Interestingly, second-order HDMR approximation does not require any knowledge of existence of multiple reference points $\mathbf{d}^1, \mathbf{d}^2, \dots, \mathbf{d}^m$ closer to the limit state/performance function. This is mainly due to the sampling performed on a plane through the reference point and thus existence of multiple reference points closer to the limit state/performance function, are taken care inherently. The estimated failure probability P_F using second-order HDMR approximation is also in good agreement with direct MCS estimate.

The effect of number of sample points used for multipoint approximation of the original limit state/performance function using FF, FS sampling schemes and second-order HDMR approximation on the reliability estimation is examined by carrying a similar analysis varying n from 3 to 9. Fig. 9(a) and Fig. 9(b) presents respectively, the variation of the reliability index β and the estimated failure probability P_F with respect to number of sample points.

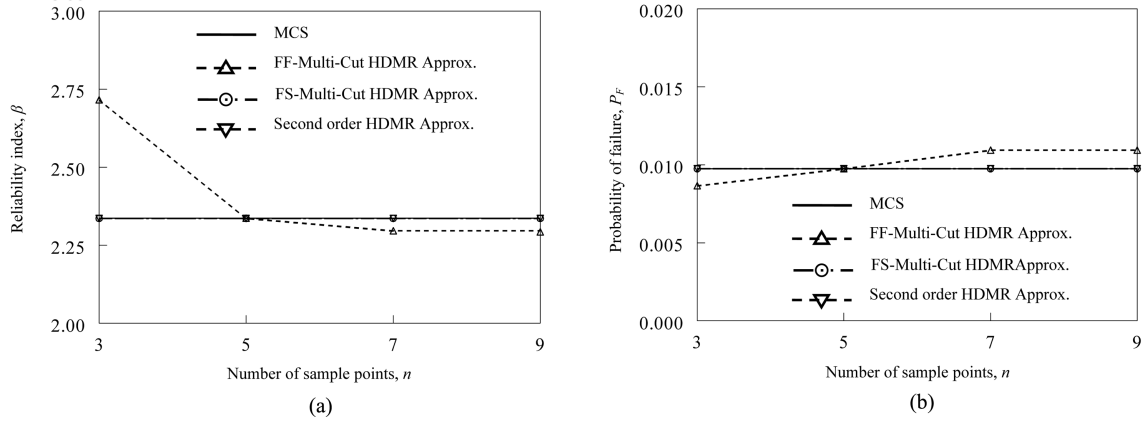


Fig. 9 Variation of reliability estimation (Example 1) (a) reliability index, β and (b) probability of failure, P_F

8.2 Example 2: two mathematical functions

The limit state/performance function of the following form with two independent standard normal variables x_1 and x_2 is considered

$$g(\mathbf{x}) = C_1 + C_2(x_1 + C_3)^r - C_4(x_1 + C_3)^2 - x_2 \tag{30}$$

C_1, C_2, C_3, C_4 are real valued parameters and r is an integer valued parameter.

Case I: $C_1 = 5, C_2 = 0.5, C_3 = 2, C_4 = 1.5, r = 3$:

Fig. 10(a) shows the limit state/performance function. This function has two design points (0, 3) and (1.62, 3.06), with two reliability indices $\beta_1 = 3$, and with $\beta_2 = 3.462$, which are obtained using RQP algorithm (Arora 2004). The proposed method in conjunction with all the four sampling schemes i.e., FF, FS, SF and SS is studied by taking $n = 7$. Using FF sampling scheme, sample point (0, 3) is identified as reference point closer to the limit state/performance function producing

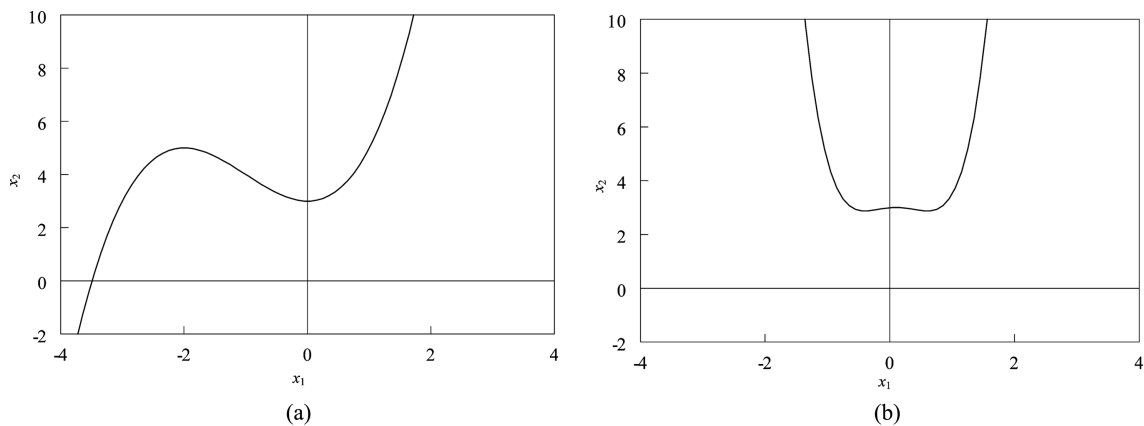


Fig. 10 Limit state function of Example 2 (a) Case I, (b) Case II

Table 4 Estimation of failure probability of Example 2 (Case I)

Method	Failure probability	Number of function evaluation ^(a)
FORM	0.001349	21
SORM (Adhikari 2004)	0.000409	188
Direct Monte Carlo simulation	0.000698	10 ⁶
Multicut-HDMR Approximation: FF sampling	0.000672	22
Multicut-HDMR Approximation: FS sampling	0.000689	52
Multicut-HDMR Approximation: SF sampling	0.000692	58
Multicut-HDMR Approximation: SS sampling	0.000698	100
Second-order HDMR	0.000696	49

^(a)Total number of times the original performance function is calculated.

^(b)Curvature fitting method is used to approximate the required curvatures of the limit-state surface.

maximum weight (obtained using Eq. (16)). Table 4 compares the failure probability estimation by different methods and associated computational efforts. A sampling size $N_S = 10^6$ is considered in direct MCS to evaluate the failure probability P_F and the COV of P_F corresponding to this sampling size is 0.038 (computed using Eq. (28)). In this example one of the design points is located along x_2 coordinate axis and the second design point is located at disparate distance (difference between two reliability indices is 0.462) from the origin. Therefore, the contribution to the failure probability estimate from the second design point is very less. The failure probability estimate by the proposed Multicut-HDMR approximation with FF sampling scheme is more accurate and efficient than either FORM or SORM and requires significantly less computational effort than direct MCS for the same accuracy. Table 4 also shows the failure probability P_F value obtained using Multicut-HDMR approximation of the original limit state/performance function with FS, SF, and SS sampling schemes and second-order HDMR approximation with $n = 7$.

Case II: $C_1 = 3, C_2 = 2, C_3 = -0.1, C_4 = 1.0, r = 4$:

Fig. 10(b) shows the limit state/performance function. For this function RQP algorithm (Arora 2004) results in two design points (0.5355, 2.9202) and (-0.2742, 2.8763), with two reliability indices $\beta_1 = 2.932$, and with $\beta_2 = 2.912$. Again the proposed method in conjunction with all the four sampling schemes i.e., FF, FS, SF and SS is studied by taking $n = 7$. Using FF sampling scheme, one sample point (0, 3) is identified as reference point closer to the limit state/performance function producing maximum weight (obtained using Eq. (16)). FF sampling scheme identifies only one sample point as reference point, due to the reason that the sample points are positioned along the coordinate axes and the limit state/performance function is almost flat along the coordinate axis x_1 . Comparison of the failure probability estimation by different methods and associated computational efforts are listed in Table 5. Compared with the benchmark result of direct MCS with COV = 0.032, the present method using FF sampling scheme provides significant accuracy to the failure probability estimation (error $\cong 0.093\%$) than FORM or SORM.

The present method using FS sampling scheme predicts the failure probability more accurately (error $\cong 0.062\%$) than the present method using FF sampling scheme at the expense of the additional computational effort. Using SF sampling scheme, one sample point (0, 3) is identified as the reference point closer to the limit state/performance function producing maximum weight

Table 5 Estimation of failure probability of Example 2 (Case II)

Method	Failure probability	Number of function evaluation ^(a)
FORM	0.001687	21
SORM (Adhikari 2004)	0.000552	188
Direct Monte Carlo simulation	0.000968	10 ⁶
Multicut-HDMR Approximation: FF sampling	0.000967	22
Multicut-HDMR Approximation: FS sampling	0.000967	52
Multicut-HDMR Approximation: SF sampling	0.000967	52
Multicut-HDMR Approximation: SS sampling	0.000967	63
Second-order HDMR	0.000948	49

^(a)Total number of times the original performance function is calculated.

^(b)Curvature fitting method is used to approximate the required curvatures of the limit-state surface.

(obtained using Eq. (16)). Inability of properly identifying the two reference point closer to the limit state/performance function, even with grid based sampling (i.e., SF sampling scheme) is due to the following reason. The x_1 coordinates of actual design points (0.5355, 2.9202) and (-0.2742, 2.8763) obtained using RQP algorithm (Arora 2004) are 0.5355 and -0.2742. The sampling schemes adopted in this study involves equally spaced sample points along each of the variable axis, or a regular grid formed by taking equally spaced sample points along each of the variable axis, The position of the sample points depends on the standard deviations σ_i of each of the random variables. In the present case, standard deviation of both the random variable is 1 and the initial reference point \mathbf{c} is taken as mean values of the random variables, which is zero. Therefore, using any of the sampling schemes, the sample points are always positioned at a minimum distance of 1 unit from each other. As x_1 coordinates of the two design points are 0.5355 and -0.2742, these two design points are within a unit distance from x_2 coordinate axis the weight functions presented in Eqs. (16) and (17) are producing only one point (0, 3) having maximum weight.

8.3 Example 3: 10-storey building with vibration absorber

Consider a 10-story shear building with a vibration absorber (VA) at the roof. The building is modelled in SAP2000 (Computers and Structures 2004) by a 10-DOF multi-linear plastic link system and the VA is modelled by a SDOF mass-spring-damper attached to the roof of the building, as shown in Fig. 11. The system is excited by random harmonic base accelerations. This problem is first studied by Der Kiureghian and Dakessian (1998) and subsequently by Gupta and Manohar (2004) in the context of illustrating the treatment of multiple design points in reliability analysis. In their study VA was modelled in such a way that, natural frequency of the system and VA coincides. But due to randomness of material and structural properties a perfect tuning would not occur in all sample realizations of the problem. Thus, depending on the relative values of the VA frequency and building frequency, the entire system could be either overtuned or undertuned. Therefore, it leads to two regions of importance in reliability estimation. The building has each floor masses m_i , ($i = 1, \dots, 10$), storey stiffnesses k_i , ($i = 1, \dots, 10$) and modal damping ratios ξ_i , ($i = 1, \dots, 10$). The VA has mass m_0 and stiffness k_0 . In the present study, all the structural parameters $m_0, \dots, m_{10}, k_0, \dots, k_{10}, \xi_0, \dots, \xi_{10}$ have been considered to be uncertain parameters along with the

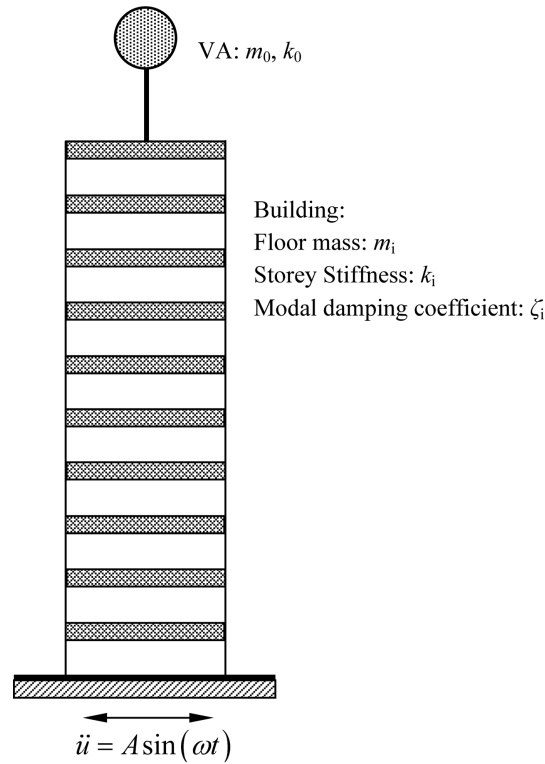


Fig. 11 10-storey building with vibration absorber

Table 6 Statistical properties of the random variables of Example 3

Random variable	m_1, \dots, m_{10}	k_1, \dots, k_{10}	m_0	k_0	ξ_0, \dots, ξ_{10}	ω
Distribution	LN	LN	LN	LN	LN	Uniform
Mean	8.75×10^4 kg	2.1×10^8 N/m	7.16×10^4 kg	3.85×10^6 N/m	0.05	[5.39-7.79]
C.O.V.	0.2	0.2	0.2	0.2	0.3	rad/s

frequency ω of the ground acceleration $A \sin(\omega t)$. Therefore, total 34 random variables are considered in the formulation of reliability problem. All the random variables are taken as independent. Statistical properties of the random variables and their distributions are presented in Table 6.

For reliability analysis we consider the limit state/performance function expressed in terms of base shear and is given by

$$g(\mathbf{x}) = V_0 - V_{Base}(\mathbf{x}) \tag{31}$$

For the mean values listed in the Table 6, the first mode frequency of the structure and the VA are identical and equal to 1.16 Hz. We also assume that threshold quantity of the base shear $V_0 = 2 \times 10^5$ kN.

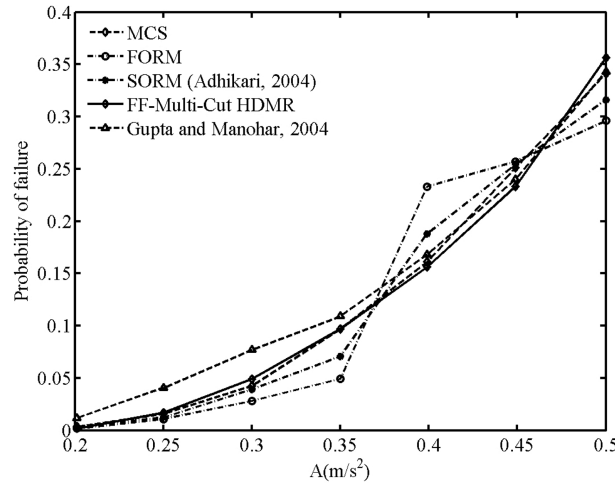


Fig. 12 Probability of failure for Example 3

To study the applicability of weight function present in this study for identification of multiple reference points closer to the limit state/performance function, FF sampling scheme is used with seven equally spaced sample points ($n = 7$) along each of the variable axis. Two sample points are identified as reference points closer to the limit state/performance function producing maximum weight (obtained using Eq. (16)). The weights of two identified points are 1.0 and 0.98. Eigenvalue analysis of 11-DOF system with the structural properties at sample point with the weight equal to 1.0 reveals the fundamental frequency of the building as 0.80 Hz and that of VA as 1.09 Hz. This situation indicates the case where VA is overtuned. Similarly, eigenvalue analysis with the structural properties at sample point with the weight equal to 0.98 reveals the fundamental frequency of the building as 1.02 Hz and that of VA as 0.68 Hz. This situation indicates the case where VA is undertuned. After identification of the two reference points closer to the limit state/performance function, local individual first-order HDMR approximations of the original limit state/performance function are constructed at the two reference points by deploying seven equally spaced sample points ($n = 7$) along each of the variable axis. Local approximations of the original limit state/performance function are blended together (using Eq. (24)) to form global approximation of the original limit state/performance function. Comparison of the estimated failure probabilities is shown in Fig. 12, for A varying from 0.2 m/s²-0.5 m/s². The results are obtained using FORM, SORM (Adhikari 2004), Multicut-HDMR approximation of the original limit state/performance function using FF sampling scheme, and direct MCS using 5000 samples. Compared with actual simulation result of MCS, the present method consistently provides accurate estimation to the failure probability, while FORM/SORM results fluctuate with the variation of A . To study the performance of the proposed method, comparative study is carried out with improved response surface method (Gupta and Manohar 2004), at $A = 0.4$ m/s². Compared with benchmark solution ($P_F = 0.1748$), FORM and SORM overestimates the failure probability by around 24.31% ($P_F = 0.2173$) and 7.15% ($P_F = 0.1873$), respectively. Multicut-HDMR approximation and improved response surface method (Gupta and Manohar 2004) underestimates the failure probability by about 4.41% ($P_F = 0.1671$) and 10.29% ($P_F = 0.1568$), respectively. However, the present method needs only 615 function evaluations, while improved response surface method (Gupta and Manohar 2004) and direct MCS

requires 14317 and 5000 number of original function evaluations, respectively. This shows the accuracy and the efficiency (in terms of original function calculations) of the multicut-HDMR approximation, over existing methods and direct MCS.

9. Conclusions

This paper presented a novel method for predicting the failure probability of structural/mechanical systems involving multiple design points. The method involves multicut-HDMR technique using multiple reference points and MLS as interpolation scheme. A new weight function is proposed for identification of multiple reference points closer to the limit surface. The failure probability is estimated by constructing multicut-HDMR approximation of the original limit state/performance function around the identified reference points.

Three numerical examples are illustrated to show the performance of the present method. Numerical examples show that the proposed method not only yields more accurate estimate of the failure probability than the alternative approximate methods (FORM/SORM) for highly nonlinear problems, but also reduces the computational effort significantly over direct MCS. Four types of sampling schemes, namely FF, FS, SF, and SS, are adopted in this study for multicut-HDMR approximation of the original limit state/performance function construction. Multicut-HDMR approximation using FF and FS sampling scheme provides desired accuracy to the predicted failure probability with least number of function evaluations. In order to reduce the approximation error further, SF and SS sampling based multicut-HDMR approximation of the original limit state/performance function could be used in reliability analysis, but the number of function evaluations increases significantly compared to FF and FS sampling. It is also observed that, second-order HDMR approximation of the original limit state/performance function does not require any knowledge of existence of multiple reference points closer to the limit state/performance function. This is mainly due to the sampling performed on a plane through the reference point and thus existence of multiple reference points closer to the limit state/performance function, are taken care inherently. A parametric study is conducted with respect to the number of sample points n used in FF and FS sampling based multicut-HDMR approximation and its effect on the estimated failure probability is investigated. An optimum number of sample points n must be chosen in approximation of the original limit state/performance function. It can be observed from the reported results in this manuscript, that $n = 5$ or 7 works well for all problems.

References

- Adhikari, S. (2004), "Reliability analysis using parabolic failure surface approximation", *J. Eng. Mech.-ASCE*, **130**(12), 1407-1427.
- Adhikari, S. (2005), "Asymptotic distribution method for structural reliability analysis in high dimensions", *P. Roy. Soc. London, Series-A*, **461**(2062), 3141-3158.
- Alis, O.F. and Rabitz, H. (2001), "Efficient implementation of high dimensional model representations", *J. Math. Chem.*, **29**(2), 127-142.
- Arora, J.S. (2004), *Introduction to Optimum Design*, Second Edition, Elsevier Academic Press, San Diego, CA.
- Au, S.K. and Beck, J.L. (2001), "Estimation of small failure probabilities in high dimensions by subset simulation", *Prob. Eng. Mech.*, **16**(4), 263-277.

- Breitung, K. (1984), "Asymptotic approximations for multinormal integrals", *J. Eng. Mech.-ASCE*, **110**(3), 357-366.
- Chowdhury, R. and Rao, B.N. (2009), "Assessment of high dimensional model representation techniques for reliability analysis", *Prob. Eng. Mech.*, **24**(1), 100-115.
- Chowdhury, R., Rao, B.N. and Prasad, A.M. (2008), "High dimensional model representation for piece wise continuous function approximation", *Comm. Numer. Meth. Eng.*, **24**(12), 1587-1609.
- Computers and Structures Inc. (2004), *CSI Analysis Reference Manual*.
- Der Kiureghian, A. and Dakessian, T. (1998), "Multiple design points in first and second-order reliability", *Struct. Saf.*, **20**(1), 37-49.
- Gavin, H.P. and Yau, S.C. (2008), "High-order limit state functions in the response surface method for structural reliability analysis", *Struct. Saf.*, **30**(2), 162-179.
- Gupta, S. and Manohar, C.S. (2004), "An improved response surface method for the determination of failure probability and importance measures", *Struct. Saf.*, **26**(2), 123-139.
- Impollonia, N. and Sofi, A. (2003), "A response surface approach for the static analysis of stochastic structures with geometrical nonlinearities", *Comp. Meth. Appl. Mech. Eng.*, **192**(37-38), 4109-4129.
- Kaymaz, I. and McMahon, C.A. (2005), "A response surface method based on weighted regression for structural reliability analysis", *Prob. Eng. Mech.*, **20**(1), 11-17.
- Lancaster, P. and Salkauskas, K. (1986), *Curve and Surface Fitting: An Introduction*, Academic Press, London.
- Li, G., Rosenthal, C. and Rabitz, H. (2001a), "High dimensional model representations", *J. Phys. Chem. A*, **105**, 7765-7777.
- Li, G., Wang, S.W. and Rabitz, H. (2001b), "High dimensional model representations generated from low dimensional data samples-I. mp-Cut-HDMR", *J. Math. Chem.*, **30**(1), 1-30.
- Liu, P.L. and Der Kiureghian, A. (1991), "Finite element reliability of geometrically nonlinear uncertain structures", *J. Eng. Mech.-ASCE*, **117**(8), 1806-1825.
- Melchers, R.E. (1989), "Importance sampling in structural systems", *Struct. Saf.*, **6**(1), 3-10.
- Rackwitz, R. (2001), "Reliability analysis-a review and some perspectives", *Struct. Saf.*, **23**(4), 365-395.
- Nair, P.B. and Keane, A.J. (2002), "Stochastic reduced basis methods", *AIAA J.*, **40**(8), 1653-1664.
- Rubinstein, R.Y. (1981), *Simulation and the Monte Carlo Method*, Wiley, New York.
- Schuëller, G.I., Pradlwarter, H.W. and Koutsourelakis, P.S. (2004), "A critical appraisal of reliability estimation procedures for high dimensions", *Prob. Eng. Mech.*, **19**(4), 463-474.
- Sobol, I.M. (2003), "Theorems and examples on high dimensional model representations", *Rel. Eng. Sys. Saf.*, **79**(2), 187-193.
- Tunga, M.A. and Demiralp, M. (2004), "A factorized high dimensional model representation on the partitioned random discrete data", *Appl. Numer. Anal. Comp. Math.*, **1**(1), 231-241.
- Tunga, M.A. and Demiralp, M. (2005), "A factorized high dimensional model representation on the nodes of a finite hyperprismatic regular grid", *Appl. Math. Comp.*, **164**, 865-883.
- Yaman, I. and Demiralp, M. (2009), "A new rational approximation technique based on transformational high dimensional model representation", *Numer. Algo.*, **52**(3), 1017-1398.
- Yonezawa, M., Okuda, S. and Kobayashi, H. (2009), "Structural reliability estimation based on quasi ideal importance sampling simulation", *Struct. Eng. Mech.*, **32**(1), 55-69.